JOURNAL OF MATERIALS SCIENCE 31 (1996) 3087–3094

Characterization of $BaO–Al_2O_3–SiO_2$ (BAS) gels during heat treatment

W. WINTER
Laboratoire de Science des Matériaux Vitreux, Université Montpellier II, U.A. CNRS No 1119, Place Eugène Bataillon Case 069, 34095 Montpellier Cedex 5, France

Gels in the system $BaO–Al_2O_3–SiO_2$ have been prepared from metal alkoxides and barium acetate. The processes during calcination and crystallization as a function of composition have been followed by means of DTA, TGA, IR and XRD. Three major regions of accelerated weight loss have been observed which correspond to the evaporation of physically adsorbed species, the oxidation of $–Al(OOCCH_3)$ and the oxidation of $Ba(OOCCH_3)_2$. The latter reactions are accompanied by strong exothermic DTA signals. The oxidation products of barium acetate tend to foam and to block the paths and channels for the oxygen supply and the removal of the volatile oxidation products, inhibiting a complete oxidation. Thus, the combustion of $Ba(OOCCH_3)_2$ is strongly dependent on the concentration, the sample volume and the heating conditions. IR shows that the gels heated up to 800 °C are structurally similar to glasses of the same composition. In all gels the metastable crystallization of hexacelsian is strongly preferred to the stable monoclinic celsian. DTA crystallization peaks appear between 960 and 1080 °C, depending on composition. In most samples hexacelsian is the only phase present, even after 5 h isothermal heat treatment.

1. Introduction

The preparation of glasses and glass–ceramics in the system $BaO–Al_2O_3–SiO_2$ (BAS) with < 40 wt % SiO_2 and > 20 wt % Al_2O_3 can be difficult due to the high melting temperatures required (> 1600 °C). The sol–gel process offers the possibility to synthesize such materials at substantially lower temperatures. Two general routes have been used so far: an all alkoxide route starting from tetraethoxysilane (TEOS), Al-s-butoxide and barium isopropoxide or a $Ba[Al(OR)_4]_2$ double alkoxide [1, 2]. This procedure has been mostly employed in order to prepare celsian and hexacelsian ($BaAl_2Si_2O_8$) ceramics [3–6]. The second route uses barium acetate as the barium precursor and has been applied for the synthesis of Ba–Si–Al–O–N oxynitride glasses, glass–ceramic matrices in composites, celsian ceramics and glass systems assigned for stainless steel substrate coatings or self-supporting substrates for VLSI chips [7–12].

One of the problems related to the use of barium acetate in sol–gel processing is the insolubility of this compound in alcohols and other organic solvents which are commonly used during sol–gel processing to overcome the immiscibility of water and alkoxides. However, as will be shown in a separate paper [12], barium acetate is soluble in mixtures of water and alcohols and the preparation of homogeneous gels without precipitation of barium acetate depends on the water-to-alcohol ratio. Addition of acetic acid increases the solubility of barium acetate.

Du *et al.* [11] have prepared several compositions in the low Al_2O_3 region of the BAS system and investigated the effects of various processing parameters on gelation time, homogeneity and calcination of the xerogels. As pointed out by the authors, it is difficult to achieve a complete oxidation and evaporation of organic material and to prevent the incorporation of residual carbon.

Gel-derived glass of stoichiometric celsian composition crystallizes at 1050–1090 °C to the metastable hexacelsian polymorph, this is the same as the melt-derived glass [13, 14]. The transformation into stable celsian is very sluggish and requires higher temperatures and several days of heating. Changing the composition towards sanbornite ($BaSi_2O_5$) encourages the crystallization of some celsian while the residual glass is resistant to sanbornite crystallization [9]. Decreasing the BaO content in glasses favours the crystallization of mullite at lower temperatures [9, 15].

In this study the gel compositions were varied systematically, while starting from the celsian composition, towards higher BaO, Al_2O_3 and SiO_2 concentrations. The objectives were to investigate the effects of heat treatment on the gels in detail, the oxidation process of residual organic material and the crystallization behaviour as a function of composition.

2. Experimental procedure

The gels have been prepared by varying systematically the BaO, Al_2O_3 or SiO_2 content when starting from the celsian composition (series B, A, S, respectively). Series M lies on the celsian–mullite tie-line. The compositions are summarized in Table I and plotted in

0022–2461

TABLE I Investigated compositions

Sample	BaO (wt %)	Al_2O_3 (wt %)	SiO_2 (wt %)
S60	44.4	29.5	26.1
CEL	40.8	27.2	32.0
S75	35.2	23.4	41.4
S85	25.7	17.1	57.2
B40	31.5	31.4	37.1
B60	50.9	22.5	26.6
M75	29.6	39.4	31.0
M50	19.1	50.9	30.0
A35	46.7	16.7	36.6
A60	35.9	35.9	28.2
A70	30.0	46.5	23.5

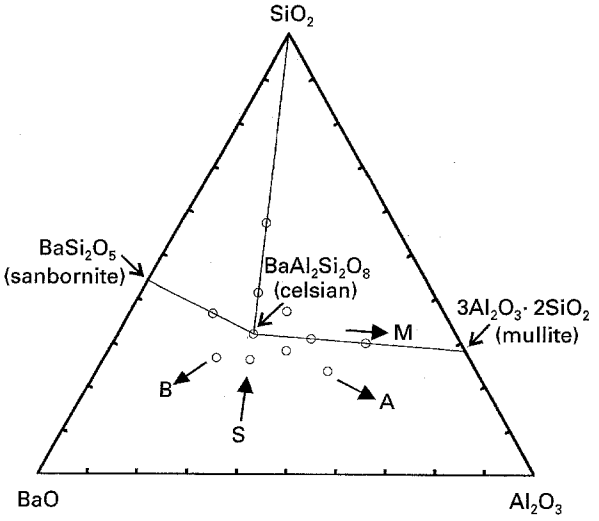

Figure 1 Investigated gel compositions in the B, A, M and S series.

Fig. 1. The details of the gel preparation are described elsewhere [12]. In brief, aluminium and silicon alkoxides and barium acetate were used in varying proportions according to the desired composition. TEOS was prehydrolysed with 1 mol/mol H_2O in ethanol. A solution of Al-sec-butoxide in 2-propanol was added to the sol and the Al-sec-butoxide modified by 1 mol/mol acetic acid. After some hours a solution of barium acetate in a calculated quantity of H_2O was added. The sol gelled within a few hours at room temperature giving rise to a homogeneous, transparent gel without any surface crystallization. After drying for 3–4 weeks the gels were ground and calcined between 200 and 700 °C for 5–20 h.

The removal of organic compounds was monitored by means of differential thermal analysis (DTA), thermogravimetric analysis (TGA) and infrared spectroscopy (IR). For DTA and TGA (Setaram) heating rates of 10 and 5 K min^{-1} were applied, respectively. Phase analysis was done on an X-ray diffractometer Philips PW1050/70 at the CuK_α wavelength.

Some gels were continuously heated up to 1000 °C at a rate of 0.4 K min^{-1} and investigated by means of infrared spectroscopy. A mixture of 1–2% gel in KBr was pressed into transparent pellets. These pellets were scanned in the infrared region 400–4000 cm^{-1} on an Fourier-transform infrared (FTIR) spectrometer (Nicolet 510P).

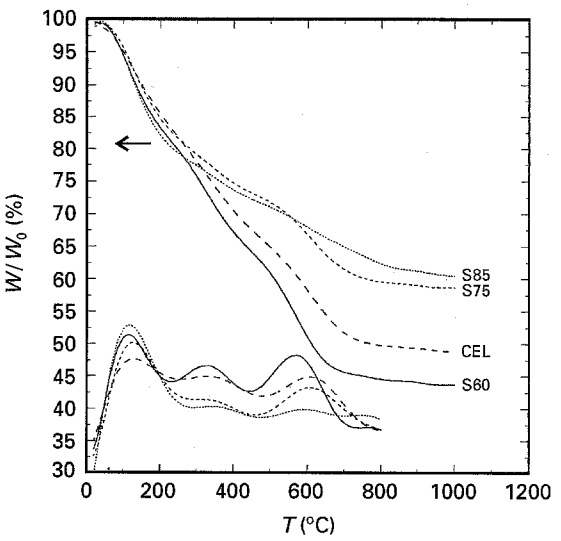

Figure 2 Weight losses and differentiated curves in the S series.

3. Results

3.1. Calcination

Heating of the prepared gels results in a weight loss of 35–55% up to 650–800 °C according to the gel composition. Above 650–800 °C the weight remains nearly constant. As valid for all samples, the TGA curves can be separated into three major domains of accelerated weight loss as expressed by the differentiated curves (Fig. 2). The minima of the differentiated curves, corresponding to a minimum in the weight loss velocity, were taken as the temperature limits of these regions. For the various gel compositions studied the range of the three regions and the corresponding maximum in the weight loss velocity differs somewhat in temperature.

A first domain with a weight loss of 12–23% appears between 70 and 220–300 °C with a maximum at 110–190 °C. The second region, extending from 220–300 °C to 435–480 °C with a maximum at 290–340 °C, comprises a weight loss of 6–18%. In this temperature range two exothermic DTA peaks appear, a strong one at 265–320 °C and a weaker one at 410–500 °C (Fig. 3, Table II). Another 7–23% decrease in mass was observed in the third region above 435–480 °C with a maximum at 565–605 °C.

Fig. 2 shows that the weight loss in the second and third region changes systematically with composition, while it is nearly independent of the gel composition in the first region. In the series S85–S75–CE–S60 the weight loss increases with increasing Al_2O_3 and BaO content or, on the basis of the precursors, acetate-modified aluminium alkoxide and barium acetate. The temperature at which the weight loss ends and the weight reaches a nearly constant level decreases between S85 and S60 from 800 to 650 °C. The linear correlation of the weight loss and the CH_3COO^- content is valid generally with $R = 0.89$ for the second and $R = 0.98$ for the third region, as depicted in Fig. 4.

The intensity of the two DTA peaks increases likewise in the S series from gel S85 to gel S60 (Fig. 3). However, the general correlation is different for the two peaks. The first peak correlates linearly with the

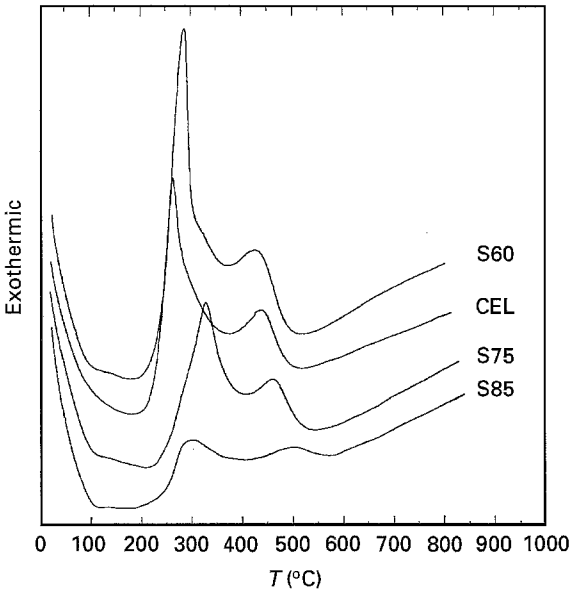

Figure 3 DTA oxidation peaks in the S series.

TABLE II Selected DTA and TGA data

Sample	1. DTA peak (°C)	2. DTA peak (°C)	End of weight loss	w/w_0 (%)
S60	288	426	650	45.3
CEL	265	438	695	50.0
S75	328	460	710	59.3
S85	303	502	800	65.0
B40	284	408	695	51.0
B60	261	451	710	53.3
M75	295	412	690	42.0
M50	293	431	680	47.2
A35	266	437	680	57.5
A60	265	441	665	53.1
A70	297	437	680	45.6

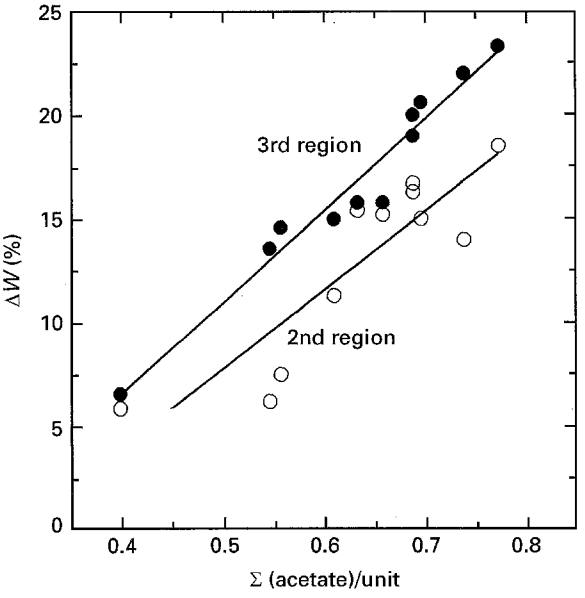

Figure 4 Weight losses in the second and third temperature regions versus total acetate content.

total acetate content ($R = 0.92$) while the second one gives a best fit with $R = 0.81$ when correlated to the barium acetate content only (Fig. 5).

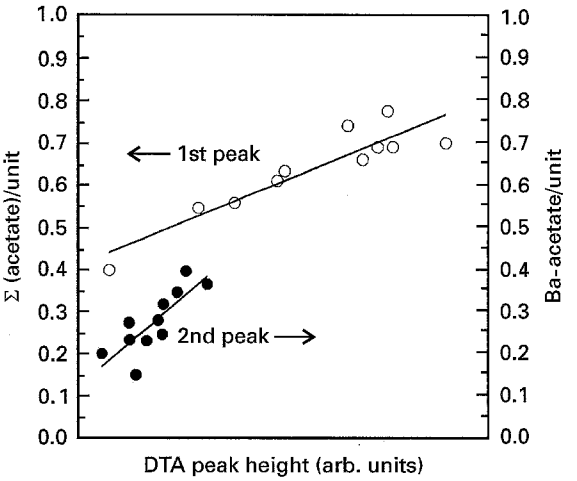

Figure 5 Total acetate and barium acetate content versus height of DTA peaks.

3.2. Infrared spectroscopy

The infrared (IR) spectra of the stoichiometric celsian composition CEL at room temperature and after heat treatment at different temperatures up to 1000 °C are plotted in Fig. 6a (3800–2400 cm^{-1}) and Fig. 6b (1800–400 cm^{-1}). Since the intermediate range contains no IR absorption bands this part has been omitted in the figures for clarity. The spectrum of the dried gel exhibits several bands due to the vibrational modes of the acetate group [16]. The strongest bands at 1571 and 1421 cm^{-1} were assigned to the symmetric and anti-symmetric stretching vibrations in the –COO group. Other bands due to different modes in barium acetate are located at 620, 655 and 1344 cm^{-1}. It is not possible to distinguish between acetate groups attached to barium or aluminium. The presence of residual alcohols is documented through the appearance of stretching and bending vibrations of C–OH and C–H at 891, 1474, 2940 and 2981 cm^{-1}. A shoulder of the anti-symmetric –COO band at 1620 cm^{-1} is attributed to the bending mode of physically adsorbed H_2O. A superposition of different modes of silanol groups and adsorbed H_2O produces a broad absorption band between 3100–3700 cm^{-1}. Three bands due to the vibrations of (Si, Al)–O in the tetrahedral network are located at about 430, 696 and 1050 cm^{-1}, the latter being rather broad.

All bands attributed to acetate disappear at 400 °C with the exception of the two most intensive peaks of the stretching vibrations in the –COO group which remain present with a strongly reduced intensity up to about 600 °C. All the bands assigned to the other organic molecules disappear likewise at a temperature of 400 °C. The maximum of the broad band between 3100–3700 cm^{-1} shifts to lower frequencies at 600 °C and disappears at 800 °C. This indicates that the chemically bonded H_2O in the silanol groups (3750–3540 cm^{-1}) is expelled between 400 and 600 °C. Due to the high porosity and high surface area of the gels heat treated to 600 °C the samples remain hydrophilic and adsorb immediately the humidity of the ambient atmosphere during storage and handling. The stretching band of the physically adsorbed H_2O is

located between 3500–3400 cm^{-1}. Heating the gels to 800 °C reduces the porosity and surface area drastically inhibiting the adsorption of greater quantities of H_2O.

At 800 °C no bands other than the three broad bands due to the tetrahedral network are observed. At 1000 °C the IR spectrum becomes better resolved, the peaks split and shift in frequencies. This expresses the increasing order in the structure due to the crystallization of hexacelsian.

3.3. Crystallization

All gels were amorphous after the drying step. X-ray diffractometry (XRD) of the samples CEL and M50 continuously heated up to 1000 °C at a rate of 0.4 K min^{-1} reveals that the gels remain amorphous up to 800–900 °C followed by crystallization of hexacelsian. The onset of crystallization was monitored by means of DTA, applying a heating rate of 10 K min^{-1} (Fig. 7). For most samples the crystallization peak of hexacelsian appears between 1060 and 1080 °C. Some compositions (S85, M50) display no peak in this temperature range, whereas others (A35, A70, S60, M50) show another exothermic peak at lower temperatures. The evolution of a second peak can be followed systematically as a function of composition in the series A and M, as evidenced by shoulders or a broadening of the main peaks in samples A60 and M75. The temperatures of the exothermic peaks and the glass transformation temperature T_g, as far as could be observed by DTA, are listed in Table III.

In order to investigate the phase composition of the crystallized gels the calcined gel powders were subjected to isothermal heat treatments at 1050 and 1250 °C for 5 h, respectively. The phase compositions for these gels as determined by XRD are listed in Table III. In all samples hexacelsian is the predominant crystalline phase. The monoclinic polymorph appears only in the samples A60, S85 and in the stoichiometric sample CEL. All other phases including mullite, $BaAl_2O_4$ and some unidentified phases represented by one or two diffraction peaks exist only in small amounts.

4. Discussion

4.1. Calcination

It is a general problem to attribute weight losses and DTA signals, observed during calcination, to specific reactions in the gels. The necessity to lead the evaporation, decomposition and oxidation of organic residues to completion before the closure of the pores in order to avoid the inclusion of residual carbon requires in many gel systems a carefully conducted calcination treatment. This problem was encountered in some of the synthesized gel compositions such as S60, A35 and A60. Organic species which have to be eliminated beside H_2O are for the major part residual alcohols (ethanol, propanol, butanol), acetate from barium acetate and acetate introduced into the sol as acetic acid in order to modify the Al-s-butoxide. The first region of accelerated weight loss up to 220–300 °C can be attributed to the evaporation of most of the alcohols and physically adsorbed H_2O.

Figs 4 and 5 show that the second and third region of weight loss as well as the two DTA peaks are predominantly the result of the decomposition and oxidation of the acetate groups. The reaction kinetics of the oxidation of $Ba[OOCCH_3]_2$ and –Al $[OOCCH_3]$ are markedly different. Fig. 8 shows the TGA and DTA plots of pure $Ba[OOCCH_3]_2$ and Al [OH] $[OOCCH_3]_2$. A broad exothermic DTA peak between 300–510 °C indicates the decomposition and oxidation of $Ba[OOCCH_3]_2$ with a maximum at 434 °C. However, the TGA experiment does not yield a substantial weight loss before a temperature of 710 °C. XRD shows that the oxidation product is $BaCO_3$. This is in accordance with the observed weight loss of 20% between 710 and 850 °C. Pure $BaCO_3$ decomposes at 1450 °C.

The decomposition of Al [OH] $[OOCCH_3]_2$ starts with the endothermic separation of the OH group at about 110 °C, accompanied by a first weight loss with a maximum at 140 °C. The acetate groups decompose at 300 °C, as indicated by a second endothermic peak, and are oxidized at 335 °C in a strong exothermic

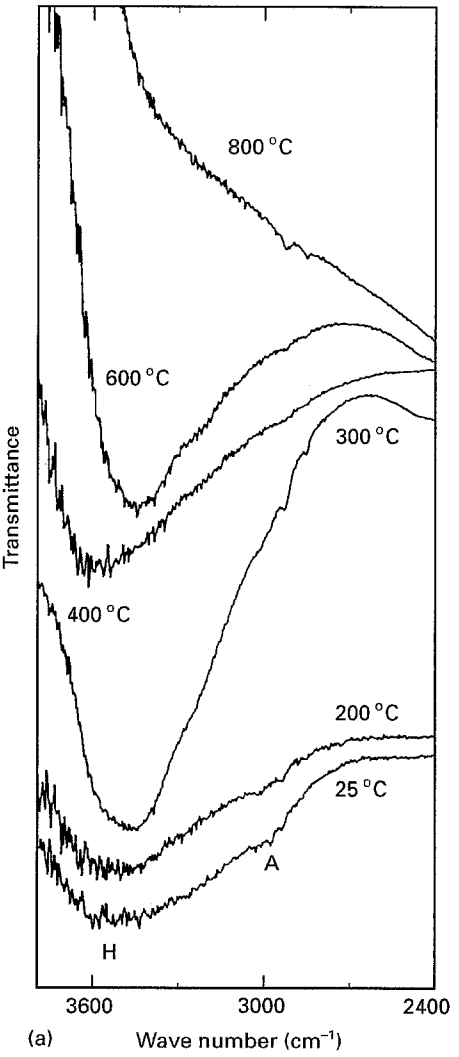

Figure 6 IR spectra of sample CEL heat treated between 25 and 1000 °C. (a) 3600–2400 cm^{-1}, (b) 1800–400 cm^{-1}. Bands from H: H_2O, B: acetate groups, A: alcohols, S: (Si, Al)–O.

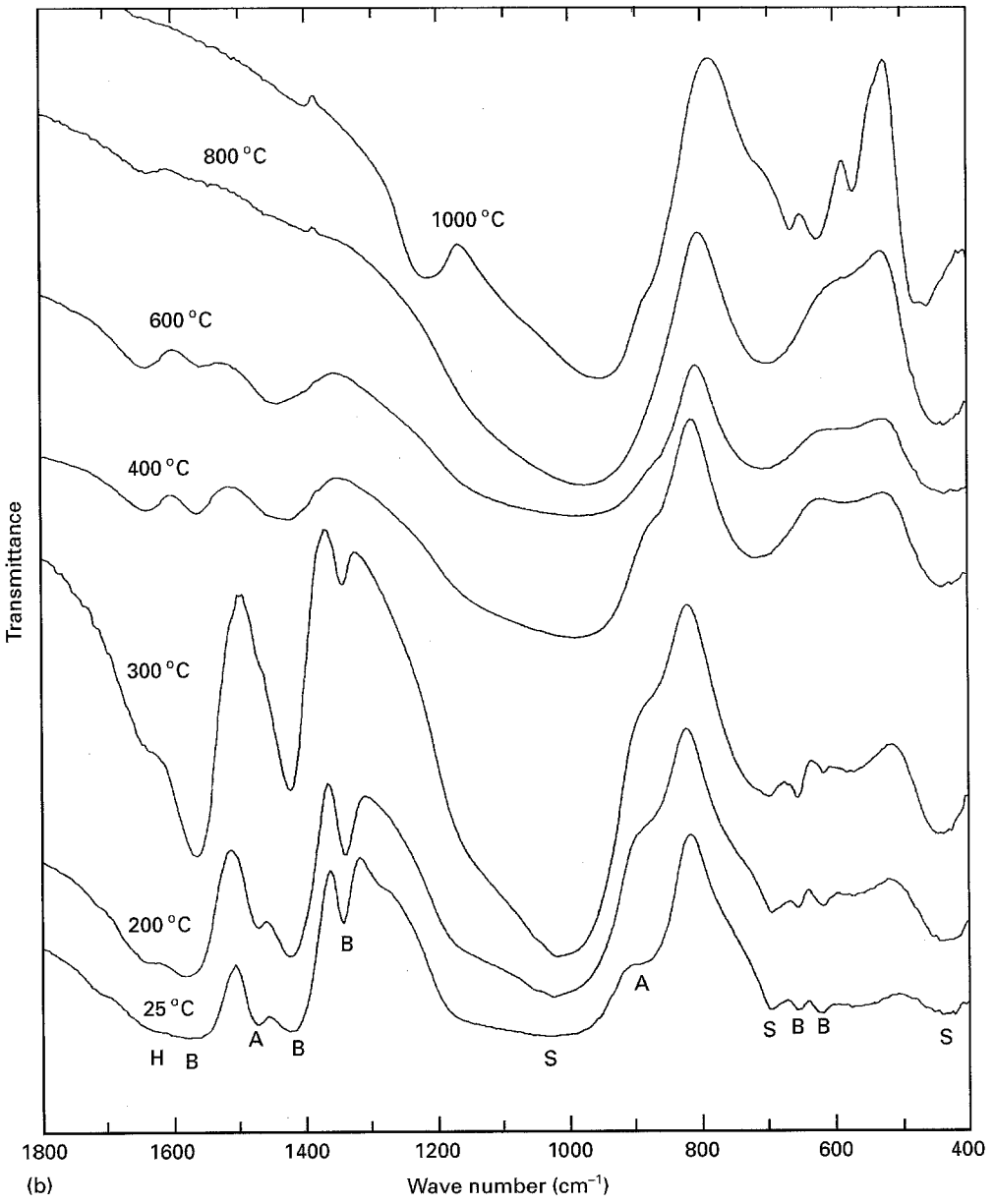

Figure 6 Continued

reaction. The corresponding weight loss starts at 280 °C and reaches its maximum at 445 °C. The total weight loss up to 700 °C corresponds to a decomposition into Al_2O_3 besides the volatile compounds.

With regard to the IR observations, the reactions in the pure products and the correlations between weight losses, DTA peak height and gel composition the following interpretations are given. The first exothermic DTA peak is a superposition of the oxidation peak of –Al $[OOCCH_3]$ and the peak of the beginning oxidation of $Ba[OOCCH_3]_2$ while the second peak is mainly the result of the oxidation of $Ba[OOCCH_3]_2$. The second region of accelerated weight loss in the TGA experiment is attributed predominantly to the oxidation of the aluminium acetate groups and, to a lesser extent, to the beginning of decomposition of $Ba[OOCCH_3]_2$. The third weight loss region is mainly due to the oxidation of $Ba[OOCCH_3]_2$.

Two points are worth noting: the existence of a substantial weight loss in the 250–450 °C region and a strong DTA peak at around 300 °C shows that a great part of –Al $[OOCCH_3]$ has not been hydrolysed and is still present in the dried gel. This fact yields an idea about the condensation rate in the gel network concerning the Al environment.

Secondly, in contrast to pure barium acetate, the oxidation of barium acetate in the gels goes to completion without formation of $BaCO_3$. In the IR spectra of gel CEL no bands due to the CO_3^{2-} anion were observed. The oxidation reaction seems to be coupled with an immediate bonding of the barium cations to the (Si, Al)-network.

While the temperature of the DTA oxidation peak of –Al$[OOCCH_3]$ (265–320 °C) is in the same temperature range as the observed weight loss (220–480 °C) this is not the case for $Ba[OOCCH_3]_2$. The weight loss due to the oxidation of $Ba[OOCCH_3]_2$ occurs at a 100–200 °C higher temperature than the correspondent DTA peaks. The same observations were made on the pure products (Fig. 8).

The discrepancy in the case of $Ba[OOCCH_3]_2$ is due to the kinetics of the oxidation reaction. As

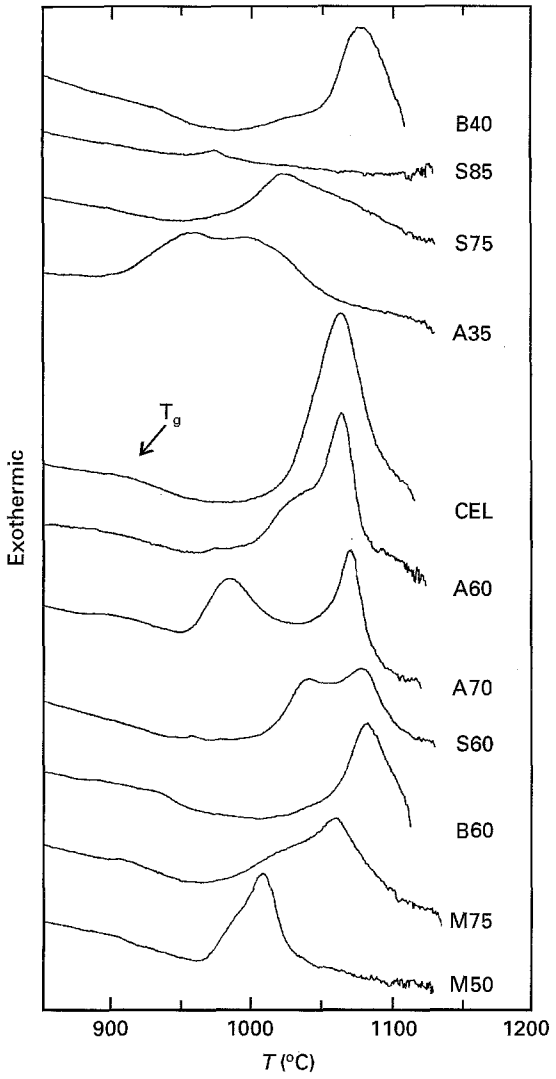

Figure 7 DTA peaks at crystallization temperatures.

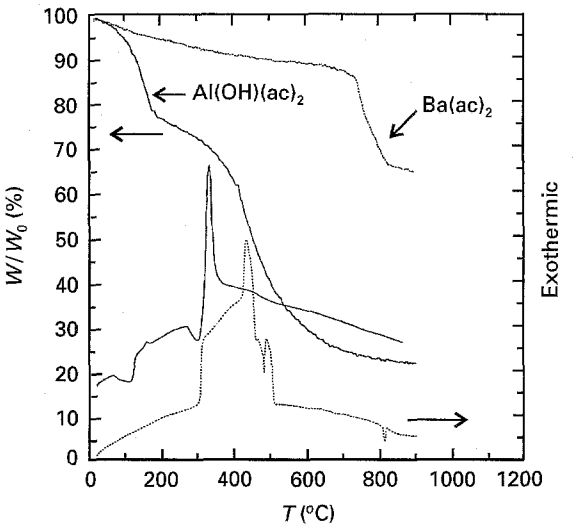

Figure 8 TGA and DTA of pure barium acetate and pure basic aluminium acetate.

observed on pure barium acetate, the powder sample begins to foam during the oxidation which possibly is related to the crystallization of $BaCO_3$ as an oxidation product. The foaming indicates that the paths and channels through which oxygen is supplied and the volatile oxidation products are removed are blocked, thus hindering further combustion. These barriers change the kinetics of the combustion process which at first are determined by open flow of material to a diffusion controlled transport mechanism through the solid material. As diffusion is much slower than open gas flow the oxidation of pure barium acetate was incomplete after the TGA experiment; this was further evidenced by the black colour of the sample.

Thus, the combustion of barium acetate is thought to be strongly dependent on the diffusion conditions in general, i.e. the oxygen supply and ventilation of the sample, the diffusion length determined by the sample volume and the barium acetate concentration and the heating rate. Thus, the much smaller mass of the DTA sample which is 1/10 that of the TGA sample explains why pure barium acetate, though foamed, is completely oxidized and white after the DTA run.

The risk of incomplete oxidation increases with increasing barium acetate concentration in the gels, essentially for the gels S60, A35 and B60. In order to avoid an incorporation of residual carbon during calcination it is especially important to apply a careful heat treatment in the temperature range 200–500 °C which is adopted according to the particular barium acetate concentration.

4.2. Infrared spectroscopy

The difference in combustion temperatures of barium acetate and aluminium acetate are not reflected by the

TABLE III T_g and crystallization peak maximum T_c from DTA and XRD of calcined gels, annealed for 5 h at 1050 and 1250 °C, respectively. C: celsian, HC: hexacelsian, M: mullite, BA_2: $BaAl_2O_4$, ?: unidentified, s: strong, m: medium, w: weak, ( ): traces.

Sample	T_g (°C)	T_c (°C)	1050 °C, 5 h	1250 °C, 5 h
S60	897	1041/1078	mHC, (BA_2)	sHC, wBA_2
CEL	907	1063	sHC, wC	sHC, wC
S75	–	1023	sHC, (?)	mHC, (?), glass
S85	–	–	glass	wHC, wC
B40	939	1075	sHC	sHC, (M)
B60	934	1082	sHC	sHC
M75	903	1060	sHC	sHC, (M)
M50	–	1008	mHC, (M)	sHC, wM
A35	810	960/995	mHC, (?)	mHC, glass
A60	885	1064	sHC, (C)	sHC
A70	865	983/1070	sHC	sHC

IR spectra. However, the sharp decrease in intensity of the 1421 and 1571 cm^{-1} bands between 300 and 400 °C is in accordance with the exothermic DTA peaks and the weight loss observed with TGA. Due to the low heating rate applied on the IR samples and sufficient oxygen supply in the open tube furnace barium acetate is completely oxidized at 600–800 °C.

At 800 °C the IR spectrum has great similarities to the spectra of alkali silicate, aluminosilicate, alkali aluminosilicate and alkaline earth aluminosilicate glasses which all show at least three bands in the 1100, 800 and 500 cm^{-1} regions [17–21]. The exact frequencies and intensities depend on the Al/Si ratio, the ratio of four-fold coordinated Al replacing Si in the network and the six-fold coordinated Al acting as modifier, and the content of glass modifiers such as alkali or alkali earth cations. Roy [17] investigated barium aluminosilicate glasses xBaO–$x$$Al_2O_3$–$(1-2x)SiO_2$ with compositions of $x = 0.05$–0.175 by IR spectroscopy. A peak in the 1100 cm^{-1} region was attributed to Si–O stretching in the tetrahedral network modified by aluminium while a peak around 800 cm^{-1} was believed to be due to the valence vibration of Al–O bonds in AlO_4 tetrahedra. A peak in the 500 cm^{-1} region is considered to be the result of a symmetric motion of bridging oxygens with only small displacement of the neighbouring cations. Location and intensity of these bands are a function of the Al/Si ratio: with increasing ratio the intensity of the 1100 cm^{-1} band decreases and that of the 800 cm^{-1} band increases while the frequencies of all three bands decrease. The latter fact is due to the increasing bond length of (Si, Al)–O and the resulting decreased force constant with increasing Al/Si ratio.

The extrapolation of the straight line expressing the linear relationship between Al/(Al + Si) and the frequency of the 1100 cm^{-1} band as documented by Roy to Al/(Al + Si) = 0.5 (celsian composition, sample CEL) yields exactly the observed frequency of 976 cm^{-1}. The locations of the two other bands follow the same tendency. In the glasses investigated it was assumed that all Al is in four-fold coordination acting as network former. The correspondence of the IR spectra with the 800 °C spectrum of sample CEL suggests that the same is true for the gel derived sample and that the structure of the gel network at 800 °C is similar to the structure of a glass with the same composition. This is also in accordance with the observed T_g of 907 °C which corresponds well with the value of 910 °C, given by Drummond and Bansal [13] for a glass of celsian composition. Consequently, the gel to glass transformation takes place between 650–800 °C in sample CEL.

4.3. Crystallization

Like in all materials of celsian composition synthesized by various other methods (powder, gel, glass) the crystallization of metastable hexacelsian is strongly preferred to the stable monoclinic compound. This is true also when the gel composition deviates considerably from $BaAl_2Si_2O_8$. During crystallization the diffusion of the atoms into their appropriate crystallographic sites is one of the determining processes. The hexacelsian structure is composed of sheets of hexagonal double rings of 12 $(Si, Al)O_4$ tetrahedra alternating with layers occupied by the barium cations in a 12-fold coordination. The tetrahedral network of celsian is more complicated. It consists of rings of four $(Si, Al)O_4$ tetrahedra and the barium cations are located in interstitial cavities in an irregular 9-fold coordination. For a cation of such a large size as barium these cavities are very narrow as is indicated by the small Ba–O distances which are in part below the sum of the ionic radii [22]. Therefore, the diffusion of the large barium cations in the celsian network into these cavities is supposed to be rather slow. On the other hand, the diffusion into the 12-coordinated sites in hexacelsian must be much easier. Another aspect supporting the crystallization of hexacelsian is given by the relatively open gel structure. As hexacelsian has a lower density (3.295 g cm^{-3}) than monoclinic celsian (3.39 g cm^{-3}) this compound is the most readily formed from gels in the central part of the system BaO–Al_2O_3–SiO_2.

As proved by XRD, the strong exothermic DTA peaks between 1060 and 1080 °C result from the crystallization of hexacelsian. The samples A70 and M50 heat treated to the temperature of the additional DTA peak at lower temperatures gave only very small XRD peaks due to hexacelsian. The origin of these DTA peaks is not very well understood presently but it must be associated with the nucleation and crystallization of hexacelsian.

The additional DTA peak at 1041 °C in the gel S60 is due to the formation of hexacelsian and some celsian. With increasing temperature the amount of hexacelsian increases strongly, as is evidenced by the second DTA peak at 1078 °C and XRD, while that of celsian remains low. The difference in the celsian and hexacelsian nucleation rates appears to be less pronounced at temperatures below 1040–1050 °C resulting in some celsian crystallization. At higher temperatures the hexacelsian nucleation rate is much higher and celsian crystallization is completely suppressed as is indicated by the total absence of celsian in the isothermally treated samples of S60.

In sample A35 the two DTA peaks are hardly resolved and rather broad in the temperature range 920–1020 °C. XRD of a DTA sample heat treated up to 970 °C yields hexacelsian whereas a sample heat treated up to 1050 °C shows increased hexacelsian peaks and peaks due to the crystallization of β-$BaSiO_3$.

The above argument about the celsian and hexacelsian nucleation rates is valid also in the case of β-$BaSiO_3$ and hexacelsian in sample A35. Like celsian in sample S60, β-$BaSiO_3$ does not appear in the isothermally annealed samples. It is interesting to note that, like hexacelsian, β-$BaSiO_3$ is metastable in this composition and, on the other hand, the stable compound $BaSi_2O_5$ never forms at the applied heating conditions.

The crystallization of hexacelsian over the large temperature range between 920 and 1020 °C is probably due to the formation of a solid solution. Hexa-

celsian can incorporate additional Si according to $2Si^{4+} = 2Al^{3+} + Ba^{2+}$ [23, 24]. When crystallized from SiO_2-rich and Al_2O_3-poor glasses the composition of the hexacelsian solid solution is dependent mainly on the temperature, i.e. the SiO_2 content increases with decreasing temperature. Thus, the DTA signal between 920–1020 °C is the result of the crystallization of β-$BaSiO_3$, a hexacelsian solid solution and the dissociation of SiO_2 with increasing temperature.

5. Conclusions

The combustion of BAS gels produced from silicon and aluminium alkoxides and barium acetate, the gel to glass conversion and the crystallization have been monitored by TGA, DTA, IR spectroscopy and XRD. The following results can be summarized:

(i) The TGA and DTA results suggest that the Al precursor modified by acetic acid is not fully hydrolysed. The oxidation of the aluminium acetate groups is indicated by a temperature range of accelerated weight loss between 250 and 450 °C and an exothermic DTA signal at 265–320 °C.

(ii) The oxidation of barium acetate occurs between 400 and 600 °C and is strongly dependent on the concentration, the sample volume and the heating conditions. Long diffusion distances in large samples and high barium acetate concentrations lead to incomplete oxidation.

(iii) The gel-to-glass conversion takes place between 650–800 °C. The IR spectrum of a sample heat treated to 800 °C indicates that the gel-derived glass structure is very similar to the structure of a melt-derived glass of the same composition.

(iv) In all compositions studied hexacelsian is the preferred crystallization product. The thermodynamically stable monoclinic celsian appears only in small amounts in the stoichiometric and in some adjacent compositions.

Acknowledgement

Professor Jean Phalippou is gratefully acknowledged for the very useful discussions on the subject and the careful reading of the manuscript.

References

1. M. CHEN, W. E. LEE and P. F. JAMES, *J. Non-Cryst. Solids* **130** (1991) 322.
2. J. C. DEBSIKDAR, *Ceram. Eng. Sci. Proc.* **14** [1–2] (1993) 405.
3. M. CHEN, W. E. LEE and P. F. JAMES, *J. Non-Cryst. Solids* **147&148** (1992) 532.
4. M. CHEN, P. F. JAMES and W. E. LEE, *J. Sol-Gel Sci. Tech.* **2** (1994) 233.
5. J. C. DEBSIKDAR, *J. Non-Cryst. Solids* **144** (1992) 269.
6. J. C. DEBSIKDAR and O. S. SOWEMIMO, *J. Mater. Sci.* **27** (1992) 5320.
7. W. K. TREDWAY and S. H. RISBUD, *J. Non-Cryst. Solids* **100** (1988) 278.
8. V. S. R. MURTHY, L. JIE and M. H. LEWIS, *Ceram. Eng. Sci. Proc.* **10** (1989) 938.
9. V. S. R. MURTHY and M. H. LEWIS, *Brit. Ceram. Trans. J.* **89** (1990) 173.
10. I. LEE and J. COVINO, *Mater. Res. Bull.* **29** (1994) 55.
11. Y.-J. DU, D. HOLLAND and R. PITTSON, *Phys. Chem. Glasses* **33** (1992) 228.
12. W. WINTER and J. PHALIPPOU, *J. Sol-Gel Sci. Tech.* to be published.
13. C. H. DRUMMOND and N. P. BANSAL, *Ceram. Eng. Sci. Proc.* **11** (1990) 1072.
14. D. BAHAT, *J. Mater. Sci.* **5** (1970) 805.
15. N. P. BANSAL and M. J. HYATT, *J. Mater. Res.* **4** (1989) 1257.
16. S. DOEUFF, M. HENRY, C. SANCHEZ and J. LIVAGE, *J. Non-Cryst. Solids* **89** (1987) 206.
17. B. ROY, *J. Amer. Ceram. Soc.* **73** (1990) 846.
18. S. A. BRAWER and W. B. WHITE, *J. Non-Cryst. Solids* **23** (1977) 261.
19. M. K. MURTHY and E. M. KIRBY, *J. Amer. Ceram. Soc.* **45** (1962) 324.
20. D. E. DAY and G. E. RINDONE, *ibid.* **45** (1962) 489.
21. J. J. VIDEAU, J. ETOURNEAU, C. GARNIER, P. VERDIER and Y. LAURENT, *Mater. Sci. Eng.* **B15** (1922) 249.
22. R. E. NEWNHAM and H. D. MEGAW, *Acta Crystallogr.* **13** (1960) 303.
23. G. OEHLSCHLEGEL, A. KOCKEL and A. BIEDL, *Glastechn. Ber.* **47** [3] (1974) 31.
24. G. OEHLSCHLEGEL, K. ABRAHAM and O. W. FLÖRKE, *Kristall und Technik* **11** (1976) 59.

Received 9 August
and accepted 21 December 1995